

Research on Engineering Structures & Materials



www.jresm.org



Melting and solidification of a PCM in a bottomheated/cooled cavity with and without metal fins

Giulia Martino, Claudia Naldi, Cesare Biserni, Sylvie Lorente

Online Publication Date: 30 December 2024

URL: http://www.jresm.org/archive/resm2024.456ma0919rs.html

DOI: http://dx.doi.org/10.17515/resm2024.456ma0919rs

Journal Abbreviation: Res. Eng. Struct. Mater.

To cite this article

Martino G, Naldi C, Biserni C, Lorente S. Melting and solidification of a PCM in a bottom-heated/cooled cavity with and without metal fins. *Res. Eng. Struct. Mater.*, 2025; 11(5): 2161-2174.

Disclaimer

All the opinions and statements expressed in the papers are on the responsibility of author(s) and are not to be regarded as those of the journal of Research on Engineering Structures and Materials (RESM) organization or related parties. The publishers make no warranty, explicit or implied, or make any representation with respect to the contents of any article will be complete or accurate or up to date. The accuracy of any instructions, equations, or other information should be independently verified. The publisher and related parties shall not be liable for any loss, actions, claims, proceedings, demand or costs or damages whatsoever or howsoever caused arising directly or indirectly in connection with use of the information given in the journal or related means.



Published articles are freely available to users under the terms of Creative Commons Attribution - NonCommercial 4.0 International Public License, as currently displayed at here (the "CC BY - NC").



Research on Engineering Structures & Materials



www.jresm.org

Research Article

Melting and solidification of a PCM in a bottom-heated/cooled cavity with and without metal fins

Giulia Martino ^{1,a}, Claudia Naldi *,1,b, Cesare Biserni ^{1,c}, Sylvie Lorente ^{2,d}

¹Department of Industrial Engineering, University of Bologna, via Risorgimento 2, 40136 Bologna, Italy ²Mechanical Engineering Department, Villanova University, 800 Lancaster Ave., Villanova, PA 19085, USA

Article Info	Abstract
Article history:	In this research, a numerical investigation is conducted using COMSOL Multiphysics to examine both melting and solidification of the PCM lauric acid,
Received 19 Sep 2024 Accepted 21 Dec 2024	placed in a vertical rectangular enclosure. The system is subjected to bottom heating and cooling, with or without metallic fins. The study focuses on evaluating the effect of the presence of metallic inclusion on the speed of the
Keywords:	phase transition front and the consequent duration of the melting and solidification processes. The presented findings are the average liquid fraction
Phase change materials; Melting; Solidification; Metal fins; Numerical study	over time, location of the phase change front, and temperature distribution within the cavity. The obtained outcomes highlight how different heat transfer processes, conductive and convective, are involved at various time instants during the PCM charging and discharging phases, as well as the heat transfer improvement yielded by the presence of metallic fins, which reduces the time needed for melting (solidification) by about 75% (86%). In addition, solid drops falling is observed when the horizontal melt layers spreading from the fin tops come in contact.
	© 2025 MIM Research Group, All rights reserved

1. Preface

Nowadays, the continuously growing energy request makes it essential to optimize the use of sustainable energy solutions. In this context, thermal energy storage (TES) systems are crucial, as they allow the link between energy generation and consumption. Indeed, in applications characterized by non-programmable energy generation, such as solar thermal systems, the adoption of appropriate storage tanks is essential for storing heat and releasing it once needed [1].

PCMs (phase change materials), have shown great potential for use in thermal energy storage systems in order to enhance the heat capacity by utilizing the latent heat of fusion during the phase transition between solid and liquid states [2,3]. Nevertheless, one of the main disadvantages of the PCMs is their low values of thermal conductivity, which inhibit the heat transfer within the material, slowing down the storage and release of heat. To overcome this disadvantage, many techniques have been proposed in the literature, such as the optimization of the PCM allocation in relation to the source of heat [4], or the coupling of PCMs with metal oxide nanoparticles [5], graphene [6], high-porosity open-cell metal foams [7], or metallic fins [8-11], to accelerate the PCM melting and solidification.

Regarding latent thermal energy storage (LTES) systems, bottom-heated LTES have been widely studied in different works [12-18]. In particular, Feng et al. [14] modeled the melting process of ice-copper nanoparticle mixtures using a new lattice Boltzmann method. Their results showed that the addition of nanoparticles of copper to the phase

^{*}Corresponding author: claudia.naldi2@unibo.it

^a orcid.org/0009-0004-7423-0121; ^b orcid.org/0000-0003-4126-8153; ^c orcid.org/0000-0003-0081-2036;

dorcid.org/0000-0002-5817-9686

change material accelerates the melting process and improves heat transfer. Similarly, a numerical investigation on a phase change material inserted in a bottom-heated square cavity during melting was performed by Gong and Mujumdar [15]. The authors used the finite element method Streamline Upwind/Petrov Galerkin, and their results revealed that a variation in the Rayleigh number leads to different flow patterns within the system. Moreover, Fteiti and Nasrallah [16] numerically studied the melting of a pure PCM in a rectangular enclosure heated/cooled from the bottom and from the top, respectively. They observed that the aspect ratio of the enclosure affects the duration of the process. In particular, if the aspect ratio is reduced, the melting process takes place faster. Parsazadeh and Duan [17] investigated the melting from the bottom of coconut oil, used as a PCM. The geometry studied is a cavity with a rectangular shape in which the PCM is confined. Their outcomes showed that the melting process takes place with two different mechanisms, depending on the Rayleigh number. In particular, the beginning of the process, characterized by small Rayleigh numbers, is dominated by heat conduction, whereas natural convection characterized by the formation of Rayleigh-Bénard cells is the heat transfer mechanism when the Rayleigh number exceeds the critical value. Also, Kousksou et al. [18] conducted a numeric analysis on the melting of gallium, inserted in a rectangular enclosure heated from a horizontal wavy surface, driven by convection. Their analysis focused on how the amplitude of the wavy bottom affects heat transfer during melting. They found that the number of Rayleigh-Bénard rolls is significantly influenced by the liquid layer height.

In this paper, a rectangular enclosure filled with a PCM, i.e. lauric acid, is numerically studied. The cavity is heated or cooled from the bottom side, whilst the other walls are adiabatic, and can include three metal fins placed from below. A specific geometry has been selected in this study in order to show the effects of the fins inclusion in a vertical enclosure, where the fins do not reach the cavity top, heated/cooled from the bottom. The behavior of the PCM during both melting and solidification is studied in order to evidence the impact of the metallic fins on the heat transfer mechanisms, duration of the melting/solidification processes, and slope of the liquid fraction trend.

2. Methods

2.1. Geometrical Configuration and Material Properties

A rectangular cavity with length A=3 cm and height B=5 cm is selected for the numerical analysis (see Fig. 1a). The enclosure contains the PCM lauric acid. Table 1 reports the main material properties.

Tahla	1 I	auric	acid	nro	perties	[1 C	ıΓ
1 able	1.1	_aui ic	atıu	טוט	perues	117	"

	Solid state	Liquid state
Temperature, T [K]	316.65	321.35
Density, ρ [kg/m ³]	940	940
Heat conductivity, λ [W/(m·K)]	0.16	0.14
Specific heat capacity, c_p [J/(kg·K)]	2180	2390
Dynamic viscosity, μ [Pa·s]		0.008
Thermal expansion coefficient, β [1/K]	0.0008	
Latent heat of fusion, L [J/kg]	187210	

The melting temperature range of the considered PCM is $\Delta T_m = 4.7$ K. The melting of the material starts at $T_m = 316.65$ K, while solidification starts at $T_s = 321.35$ K. Two distinct scenarios are examined: only the PCM is present in the cavity; also 3 aluminum fins ($\lambda_{fins} = 3.00$).

237 W/(m·K), ρ_{fins} = 2700 kg/m³, c_{pfins} = 897 J/(kg·K)) are included. The fins are attached to the cavity bottom and shorter than the enclosure (see Fig. 1b). The width and height of the fins are respectively w = 0.1 cm and h = 3.5 cm, while the spacing between fins is s = 1.4 cm. It is important to note that the fins located in correspondence of the cavity lateral sides have a width halved with respect to that of the central fin, to minimize the boundary influence.

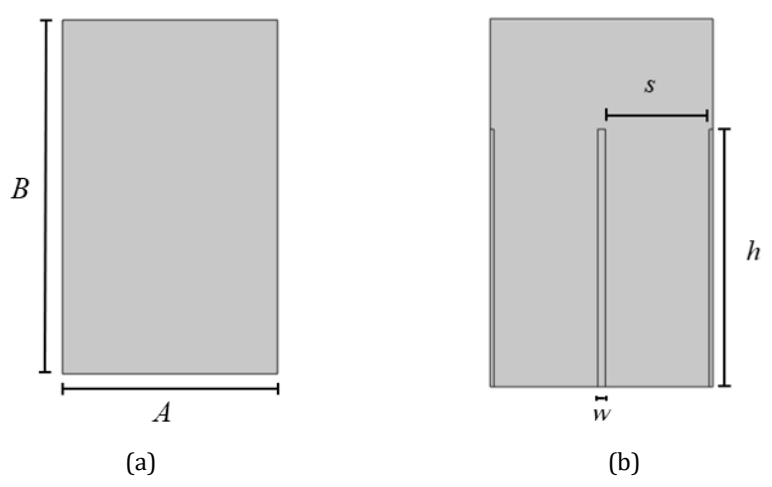


Fig. 1. Studied geometry: vertical enclosure without (a), or with (b) fins

2.2. Numerical Method

To simulate the melting and solidification processes of lauric acid, contained within the cavity, with and without fins, the top and lateral surfaces of the enclosure are considered adiabatic, whereas the bottom wall is maintained at a fixed temperature. In particular, throughout melting, the cavity is bottom-heated at T_H , which is determined as the sum of the melting temperature T_m , and a constant value ΔT_P , that is equal to 37.35 K:

$$T_{H} = T_{m} + \Delta T_{n} \tag{1}$$

In this case, an initial temperature equal to T_m is assumed for the entire domain, ensuring that the lauric acid is in the solid phase. Similarly, the solidification process is conducted by setting the bottom side of the cavity at a fixed temperature value equal to T_c , defined as the difference between the solidification temperature T_s , and the constant value ΔT_p :

$$T_{c} = T_{s} - \Delta T_{p} \tag{2}$$

For the solidification process, the initial temperature is T_s in the whole domain, ensuring that the lauric acid is in the liquid phase. Furthermore, the phase change material in the liquid state is considered incompressible, the flow is assumed to be laminar (Boussinesq approximation is adopted), PCM and metallic inclusions exhibit isotropic properties. The governing equations consist of the conservation of mass, momentum, and energy:

$$\nabla \Box \vec{r} = 0 \tag{3}$$

$$\rho \frac{\partial \vec{v}}{\partial \tau} + \rho \left(\vec{v} \Box \nabla \right) \vec{v} = -\nabla p + \mu \nabla^2 \vec{v} + \rho \vec{g} - \vec{g} \beta \rho \left(T - T_m \right) \theta \tag{4}$$

$$\frac{\partial T}{\partial \tau} + (\vec{v} \Box \nabla) T = \frac{\lambda}{\rho c_{p,m}} \nabla^2 T \tag{5}$$

where \vec{v} is the velocity vector, p is pressure, \vec{g} is the gravity acceleration vector, τ is time, θ is the PCM local liquid fraction, and $c_{p,m}$ is the modified specific heat capacity. In particular, the latter is defined in agreement with the apparent heat capacity method as follows [20]:

$$c_{p,m} = c_p$$
 if $T < T_m$ or $T > T_s$ (solid and liquid state) (6)

$$c_{p,m} = c_p + \frac{L}{\Delta T_m}$$
 if $T_m < T < T_s$ (mushy region) (7)

where L is the PCM latent heat of fusion. Furthermore, θ is a dimensionless parameter that quantifies the fraction of liquid present. In detail, θ assumes the following values:

$$\theta = 0 \text{ if } T < T_m \text{ (solid state)}$$
 (8)

$$\theta = \frac{T - T_m}{\Delta T_m} \text{ if } T_m < T < T_s \text{ (mushy region)}$$
(9)

$$\theta = 1 \text{ if } T > T_c \text{ (liquid state)}$$
 (10)

In the case with the aluminum fins attached to the cavity bottom, heat transfer through the fins is due to conduction:

$$\rho_{\text{fins}} c_{p,\text{fins}} \frac{\partial T}{\partial \tau} = \lambda_{\text{fins}} \nabla^2 T \tag{11}$$

The boundary conditions regarding the melting and solidification processes are reported in Eqs. (12)-(14) and Eqs. (12)-(13), (15), respectively. The initial conditions for the melting process are expressed by Eqs. (16)-(17), whereas those for the solidification one by Eqs. (16), (18):

$$\vec{v}(0, y, \tau) = \vec{v}(A, y, \tau) = \vec{v}(x, 0, \tau) = \vec{v}(x, B, \tau) = 0$$
(12)

$$\frac{\partial T}{\partial x}\Big|_{x=0} = \frac{\partial T}{\partial x}\Big|_{x=A} = \frac{\partial T}{\partial y}\Big|_{y=B} = 0 \tag{13}$$

$$T(x,0,\tau) = T_{\mu} \tag{14}$$

$$T(x,0,\tau) = T_c \tag{15}$$

$$\vec{v}(x,y,0) = 0 \tag{16}$$

$$T(x,y,0) = T_{m} \tag{17}$$

$$T(x,y,0) = T_c \tag{18}$$

The equations were solved using the finite element software COMSOL Multiphysics.

2.3. Mesh Sensitivity Analysis

An unstructured grid with triangles as elements is used for the discretization of the domain. Along the walls and the fins, a boundary layer mesh is included, to optimize the grid for laminar flow. To verify the independence of the results from the grid, three distinct

meshes are considered. The average liquid fraction values over time for the PCM melting in the cases with and without fins, obtained with the three grids, are compared by considering maximum absolute error and root mean square error (RMSE), as shown in Table 2.

Table 2. Results of the mesh sensitivity analysis: average liquid fraction errors

	Cavity without fins			Cavity with three fins		
Grid	Element count	Maximum absolute error	RMSE	Element count	Maximum absolute error	RMSE
First Grid	5742	0.0213	0.0120	6117	0.1012	0.0109
Second Grid	5970	0.0096	0.0044	7601	0.0168	0.0013
Third Grid	6378	-	-	8412	-	-

In addition, the height of the phase change front as a function of time, evaluated in the middle of the cavity without fins with the three different meshes, is compared for both the melting (see Fig. 2a) and solidification (see Fig. 2b) processes.

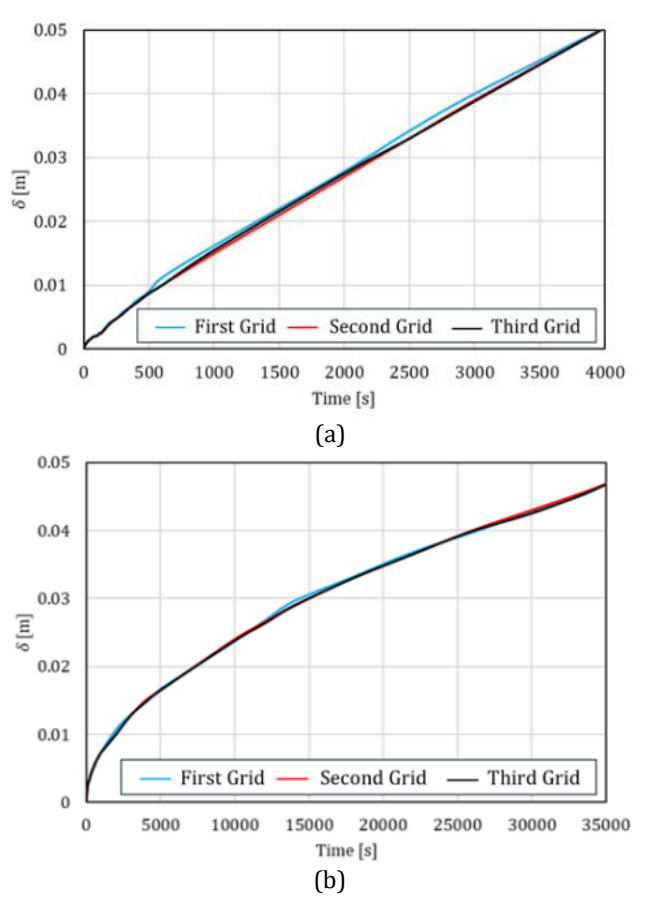


Fig. 2. Results of the mesh sensitivity analysis: melting (a) and solidification (b) front height as a function of time in the middle of the cavity without fins

Due to the very low values of the errors, in terms of average liquid fraction, obtained by the Second Grid (see Table 2) and to the negligible difference between the phase change front position obtained with the Second Grid with respect to the Third Grid (see Fig. 2), the mesh with 5970 elements is adopted.

2.4. Model Validation

The model used in this study is validated against the results presented by Shokouhmand and Kamkari [21] for the melting process, and against the results presented by Kiyak et al. [22] for the solidification process. Shokouhmand and Kamkari [21] studied experimentally the temperature distribution and the progression of the melting front of lauric acid contained in a vertical rectangular heat storage with one-side heating. In particular, they performed many experimental runs by heating the right wall at various constant temperature values, providing benchmark data to validate numerical codes.

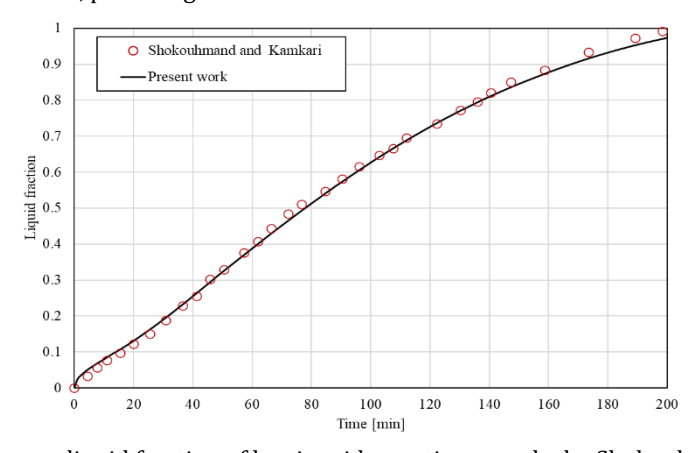


Fig. 3. Average liquid fraction of lauric acid over time, results by Shokouhmand and Kamkari [21] and by the present model

The average liquid fraction trend obtained with the proposed method and that yielded by the experiment of Shokouhmand and Kamkari in the case of a constant wall temperature equal to 70 °C is shown in Fig. 3. Moreover, the melting front position at some instants yielded by the proposed method and by the experiment of Shokouhmand and Kamkari [21] is compared in Fig. 4. A good agreement is observed between the results of this work and those obtained in Ref. [21]. The maximum absolute error in the average liquid fraction values is 0.0206 and the RMSE is 0.0114, while the maximum discrepancy between the melting front position obtained by this model and by Shokouhmand and Kamkari [21] is 0.0027 m.

Kiyak et al. [22] numerically studied the performance of thermal energy storage units filled with PCM. The investigation was assessed for the melting and solidification processes of the PCM RT42, considering the influences of the heater and cooler positions (bottom, top, and side) and the impact of the geometry shape (square and circular). Fig. 5 shows the average liquid fraction trend obtained by this model with that yielded by Kiyak et al. [22] in the case of cooling of RT42 confined within a square cavity cooled from the bottom. A good agreement can be found between the results of this study and those reported in Ref. [22]: the maximum absolute error in the average liquid fraction is 0.0175, and the RMSE is 0.0112. Furthermore, Fig. 6 compares the solidification front position within the square cavity at different time instants, as determined by the proposed method and by Kiyak et al. [22]. A good agreement can be observed: the maximum difference between the solidification front height obtained by this model and that of Ref. [22] is equal to 0.0020 m.

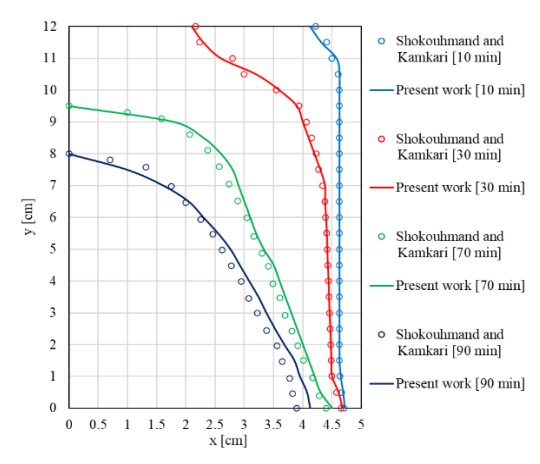


Fig. 4. Melting front evolution at different times, results by Shokouhmand and Kamkari [21] and by the present model

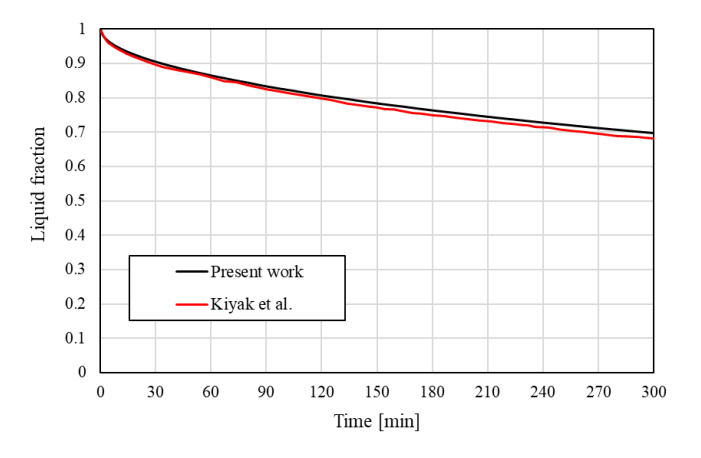


Fig. 5. Average liquid fraction of RT42 over time, results by Kiyak et al. [22] and by the present model

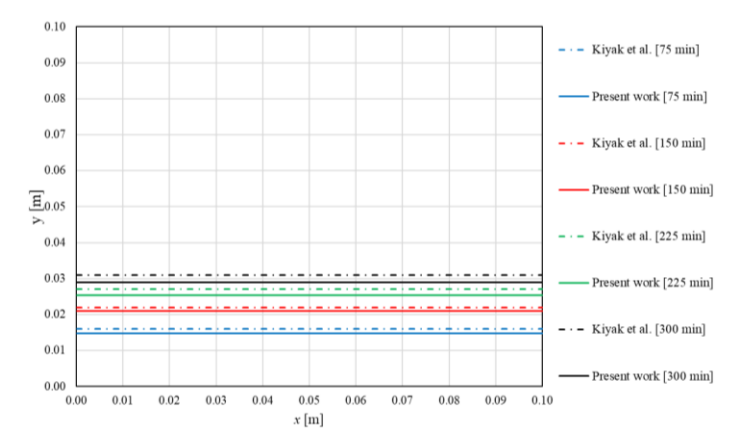


Fig. 6. Solidification front evolution at different times, results by Kiyak et al. [22] and by the present model

3. Results and Discussion

The average liquid fraction values, obtained for the PCM melting and solidification in the cavity with and without fins, are shown as a function of time in Figs. 7-8. It is noticeable how the use of metal fins leads to a significant reduction in the time required to conclude the melting process of lauric acid (average liquid fraction of 1 in Fig. 7), because they enhance the phase change by conveying heat from the bottom to the top of the cavity. Specifically, the melting time is about 4458 s for the cavity without fins, while it is only about 1095 s in the case with fins, which means a reduction of about 75%.

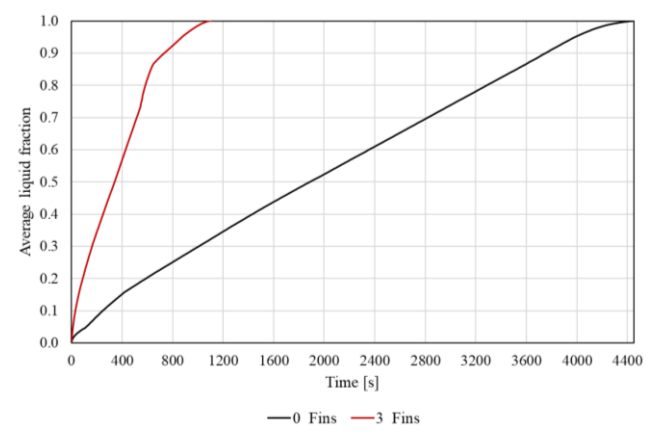


Fig. 7. Average liquid fraction for the lauric acid melting, cavity with/without fins

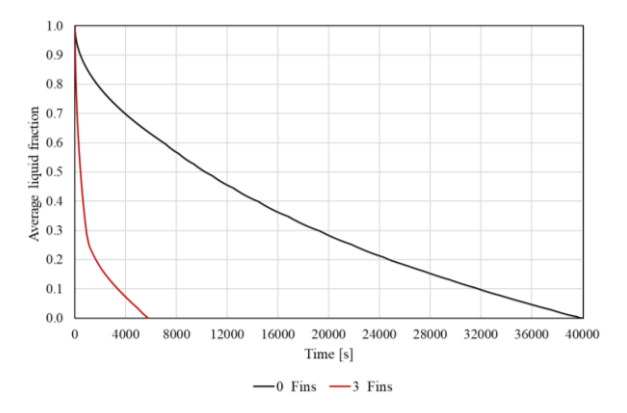


Fig. 8. Average liquid fraction for the lauric acid solidification, cavity with/without fins

The use of fins allows a significant reduction in the solidification time as well, as evident by comparing the red and black curves in Fig. 8. In particular, a reduction in the solidification time of about 86% is observed: from 40075 s in the absence of fins to 5793 s when 3 fins are added (average liquid fraction equal to 0 in Fig. 8).

It is worth noting that the PCM solidification is significantly longer than the melting. The formation of convective cells, in fact, accelerates the melting. The solidification process, on the other hand, is governed by the conductive regime only (bottom-cooled enclosure), resulting in much longer times needed to finish the transition from liquid to solid. More in detail, the PCM melting process is initially dominated by thermal conduction, whereas, subsequently, Rayleigh–Bénard cells begin to develop, triggering a shift in the heat transfer mechanism from a conductive regime to a natural convective one [23].

Fig. 9 shows the time sequence of temperature distribution and streamlines in the case of melting without fins: at the beginning ($\tau = 50$ s in Fig. 9) the melting front is planar (conductive regime), but when the convective regime turns out to be more effective to transfer heat from the enclosure bottom, Rayleigh–Bénard cells begin to develop ($\tau = 135$ s in Fig. 9), then the rolls become bigger and less numerous ($\tau = 800$ s in Fig. 9).

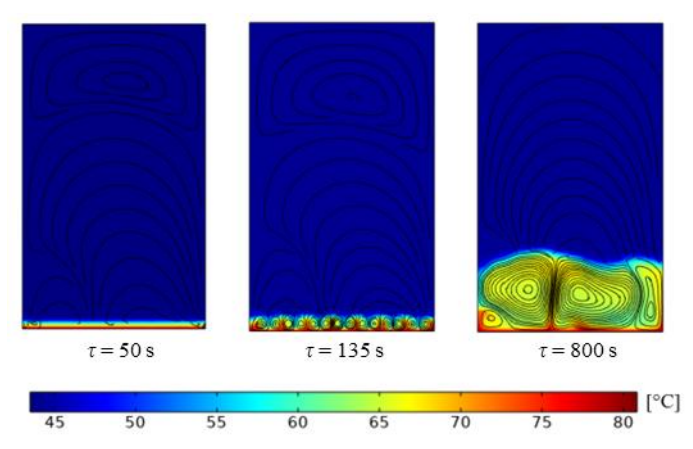


Fig. 9. Progression of lauric acid melting without fins: $\tau = 50$ s (conductive regime), $\tau = 135$ s (transition from conduction to convection), $\tau = 800$ s (convective regime)

Fig. 10 shows the liquid layer thickness δ over time during the melting process in the cavity without fins, evaluated at the enclosure center. It is evident how the evolution of δ follows two different trends: during the initial part of the process, δ is proportional to $\tau^{0.5}$, then to τ , in agreement with the theoretical results [23]. Moreover, the transition between conduction to the convection is highlighted in Fig. 10 by the inflection on the curve, which matches the theoretical analysis predictions: τ = 134.92 s and δ = 0.0019 m (see the black lines in Fig. 7).

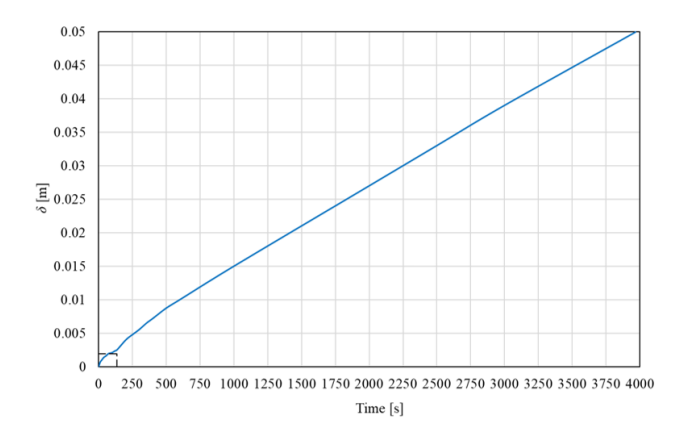


Fig. 10. Liquid layer thickness versus time; cavity without fins

Fig. 11 shows the progression of lauric acid melting in the presence of fins. In this case, the melting process occurs simultaneously from the cavity bottom and from the fins, which are heated up to the temperature T_H very soon. After a brief phase where the PCM is heated by conduction from the fins and from the bottom wall, Rayleigh–Bénard cells develop in the bottom space between two adjacent fins, as well as convective cells along the fins (see Fig. 11, left). As the heating process continues, the cells formed along the fins tend to enlarge

at the fin top and to merge, generating drops of solid material at the center between consecutive fins (see Fig. 11, middle). The convective cells exhibit a descending liquid movement at the boundary with the solid phase, so that the shear forces drive the solid drop downward to the cavity base, where the solid material completes its melting (note that the density of the material in both phases is the same). Additionally, convective cells also develop from the fins top, and combine with the vertical cells developed along the fins (that now fill the entire spacing between fins, see Fig. 11, right). These new rolls help melt the PCM located at the enclosure top, which is not reached by the metallic fins. Indeed, the melting of the material above the fins is slower, as highlighted by the decreased slope of the final part of the red curve in Fig. 7.

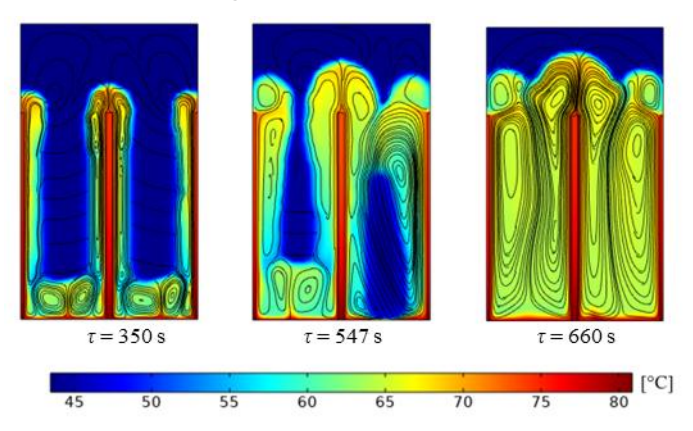


Fig. 11. Progression of lauric acid melting with fins: $\tau = 350$ s (rolls formation), $\tau = 547$ s (solid drops falling), $\tau = 660$ s (cells merged)

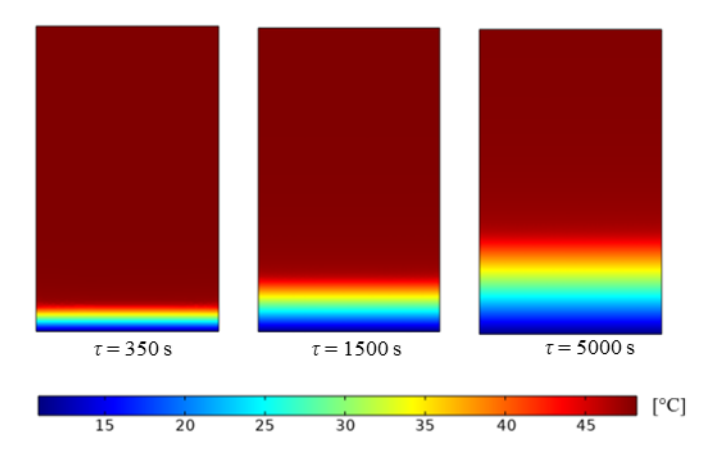


Fig. 12. Progression of lauric acid solidification without fins

Figs. 12-13 show the progression of the solidification of lauric acid in the absence/presence of fins, respectively. It is evident that in this case, the conditions for the formation of convective cells are not present. Therefore, the solidification process occurs solely through the conduction regime, in agreement with the literature [24]. As a result, the solidification times are much longer than the melting ones (by about 5-9 times). However, the inclusion of fins accelerates the PCM solidification (compare temperature distributions at corresponding time instants in Figs. 12-13), but when the phase transition front arrives at the upper part of the fins, the process slows down, as captured by the slope change in the red curve of Fig. 8. Fig. 14 shows the vertical position δ' of the phase change

front versus time in the case of solidification in the cavity without fins, evaluated at the enclosure center. The time evolution of δ' is proportional to $\tau^{0.5}$, without any change in the curve slope, consistently with the conduction-dominated regime of the phase change.

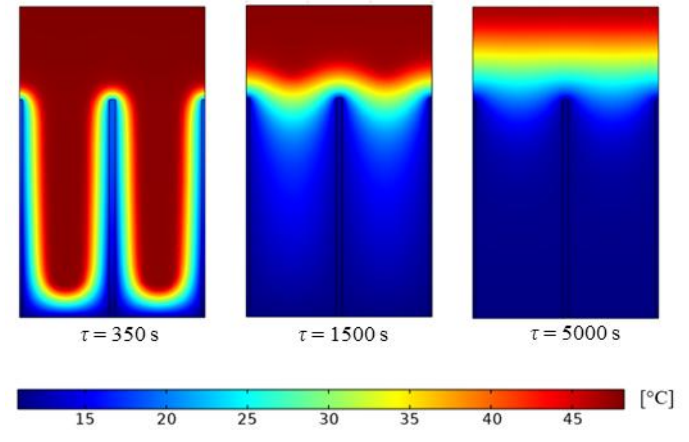


Fig. 13. Progression of lauric acid solidification with fins

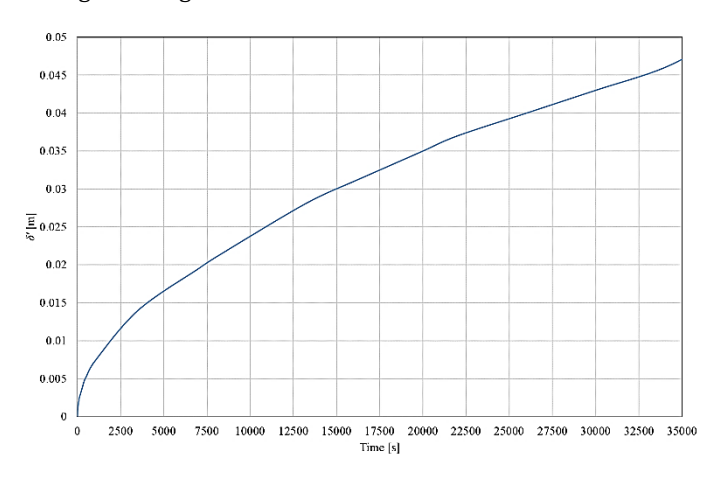


Fig. 14. Solid layer thickness versus time; cavity without fins

4. Conclusions

In this paper, a computational study is performed on the phase transition from solid to liquid, and vice versa, of lauric acid used as PCM. The material is confined within a rectangular cavity, with and without metallic fins, and is heated or cooled from the bottom, while the other walls of the enclosure are adiabatic.

The performance of the system during both melting and solidification is numerically analyzed in order to highlight the influence of the presence of the metallic fins on the heat transfer typology (namely, conduction or convection), speed of the phase change front, and duration of the melting/solidification process in a vertical rectangular enclosure with fixed geometry and temperature values of the bottom side. The governing equations are solved through the commercial software COMSOL Multiphysics and both mesh sensitivity analysis and validation of the model against literature results have been performed.

The obtained results evidence how, without fins, the melting of the PCM takes place due to a combination of an initial conductive regime, and a subsequent convective regime with the development of Rayleigh–Bénard cells. Specifically, when convection is more efficient in the heat transfer from the enclosure bottom with respect to conduction, convective cells start to develop, enhancing the PCM melting. In contrast, the solidification process occurs only through thermal conduction, with consequent longer times to complete the phase change.

If metal fins are attached to the bottom side of the enclosure, also convective cells develop vertically along the fins during the melting process. Then solid drops are created, due to the progression of the melting front spreading in the horizontal direction from the upper part of the fins. The shear forces due to the convective rolls push the solid drops toward the cavity bottom, where they end up melting. In addition, convective cells develop from the fins top and combine with the cells along the fins, enhancing the fusion of lauric acid located at the enclosure top, which is not reached by the metallic fins. The presence of high-conductivity inserts can reduce the duration of melting and solidification processes respectively by 75% and 86%.

Acknowledgement

The authors acknowledge that this study is supported by the National Recovery and Resilience Plan (NRRP), Mission 4 Component 2 Investment 1.3 - "Creazione di "Partenariati estesi alle università, ai centri di ricerca, alle aziende per il finanziamento di progetti di ricerca di base"" of Italian Ministry of University and Research funded by the European Union - NextGenerationEU; Project code PE0000021, "Network 4 Energy Sustainable Transition (NEST)", Spoke 5 (Energy Conversion), CUP J33C22002890007, and by the the Emilia-Romagna Regional Development Fund PR-FESR 2021-2027 Program under the project SACER - Sviluppo e integrazione di Accumuli innovativi nelle Comunità Energetiche Rinnovabili, CUP J47G22000760003.

References

- [1] Ali HM, Rehman T, Arıcı M, Said Z, Durakovi'c B, Mohammed HI, Kumarj R, Rathod MK, Buyukdagli O, Teggarl M. Advances in thermal energy storage: Fundamentals and applications. Progress in Energy and Combustion Science, 2024; 100: 101109. https://doi.org/10.1016/j.pecs.2023.101109
- [2] Sharma A, Tyagi VV, Chen CR, Buddhi D. Review on thermal energy storage with phase change materials and applications. Renewable and Sustainable Energy Reviews, 2009; 13: 318-345. https://doi.org/10.1016/j.rser.2007.10.005
- [3] Tao YB, He Y. A review of phase change material and performance enhancement method for latent heat storage system. Renewable and Sustainable Energy Reviews, 2018; 93: 245-259. https://doi.org/10.1016/j.rser.2018.05.028
- [4] Lorente S, Bejan A, Niu JL. Phase change heat storage in an enclosure with vertical pipe in the center. International Journal of Heat and Mass Transfer, 2014; 72: 329-335. https://doi.org/10.1016/j.ijheatmasstransfer.2014.01.021
- [5] Khan Z, Khan ZA, Sewell P. Heat transfer evaluation of metal oxides based nano PCMs for latent heat storage system application. International Journal of Heat and Mass Transfer, 2019; 144: 118619. https://doi.org/10.1016/j.ijheatmasstransfer.2019.118619
- [6] Kant K, Shukla A, Sharma A, Biwole PH. Heat transfer study of phase change materials with graphene nano particle for thermal energy storage. Solar Energy, 2017; 146: 453-463. https://doi.org/10.1016/j.solener.2017.03.013
- [7] Cui W, Si T, Li X, Li X, Lu L, Ma T, Wang Q. Heat transfer enhancement of phase change materials embedded with metal foam for thermal energy storage: A review. Renewable

- and Sustainable Energy Reviews, 2022; 169: 112912. https://doi.org/10.1016/j.rser.2022.112912
- [8] Al-Omari SAB, Qureshi ZA, Elnajjar E, Mahmoud F. A heat sink integrating fins within high thermal conductivity phase change material to cool high heat-flux heat sources. International Journal of Thermal Sciences, 2022; 172: 107190. https://doi.org/10.1016/j.ijthermalsci.2021.107190
- [9] Acir A, Canlı ME. Investigation of fin application effects on melting time in a latent thermal energy storage system with phase change material (PCM). Applied Thermal Engineering, 2018; 144: 1071-1080. https://doi.org/10.1016/j.applthermaleng.2018.09.013
- [10] Shukla A, Kant K, Biwole PH, Pitchumani R, Sharma A. Melting and solidification of a phase change material with constructal tree-shaped fins for thermal energy storage. Journal of Energy Storage, 2022; 53: 105158. https://doi.org/10.1016/j.est.2022.105158
- [11] Kirincic M, Trp A, Lenic K, Torbarina F. Numerical analysis of the influence of geometry parameters on charging and discharging performance of shell-and-tube latent thermal energy storage with longitudinal fins. Applied Thermal Engineering, 2024; 236: 121385. https://doi.org/10.1016/j.applthermaleng.2023.121385
- [12] Yanga XH, Tana SC, Dinga YJ, Wanga L, Liua J, Zhoua YX. Experimental and numerical investigation of low melting point metal based PCM heat sink with internal fins. International Communications in Heat and Mass Transfer, 2017; 87: 118-124. https://doi.org/10.1016/j.icheatmasstransfer.2017.07.001
- [13] Satbhai O, Roy S. Criteria for the onset of convection in the phase-change Rayleigh-Bénard system with moving melting-boundary. Physics of Fluids, 2020; 32: 064107. https://doi.org/10.1063/5.0004979
- [14] Feng Y, Li H, Li L, Bu L, Wang T. Numerical investigation on the melting of nanoparticle-enhanced phase change materials (NEPCM) in a bottom-heated rectangular cavity using lattice Boltzmann method. International Journal of Heat and Mass Transfer, 2015; 81: 415-425. https://doi.org/10.1016/j.ijheatmasstransfer.2014.10.048
- [15] Gong ZX, Mujumdar AS. Flow and heat transfer in convection-dominated melting in a rectangular cavity heated from below. International Journal of Heat and Mass Transfer, 1998; 41: 2573-2580. https://doi.org/10.1016/S0017-9310(97)00374-8
- [16] Fteiti M, Nasrallah SB. Numerical study of interaction between the fluid structure and the moving interface during the melting from below in a rectangular closed enclosure. Computational Mechanics, 2005; 35: 161-169. https://doi.org/10.1007/s00466-004-0597-6
- [17] Parsazadeh M, Duan X. Numerical and experimental investigation of phase change heat transfer in the presence of Rayleigh-Benard convection. ASME Journal of Heat and Mass Transfer, 2020; 142: 062401. https://doi.org/10.1115/1.4046537
- [18] Kousksou T, Mahdaoui M, Ahmed A, Msaad AA. Melting over a wavy surface in a rectangular cavity heated from below, Energy, 2014; 64: 212-219. https://doi.org/10.1016/j.energy.2013.11.033
- [19] Zhang X, Lorente S, Wemhoff AP. Modeling the thermal energy storage capability of a phase change material confined in a rectangular cavity. International Communications in Heat and Mass Transfer, 2021; 126: 105367. https://doi.org/10.1016/j.icheatmasstransfer.2021.105367
- [20] Naldi C, Dongellini M, Morini GL. The evaluation of the effective thermal conductivity of metal-foam loaded phase change materials. Journal of Energy Storage, 2022; 51: 104450. https://doi.org/10.1016/j.est.2022.104450
- [21] Shokouhmand H, Kamkari B. Experimental investigation on melting heat transfer characteristics of lauric acid in a rectangular thermal storage unit. Experimental

- Thermal and Fluid Science, 2013; 50: 201-212. https://doi.org/10.1016/j.expthermflusci.2013.06.010
- [22] Kiyak B, Oztop H. F, Biswas N, Selimefendigil F. Effects of geometrical configurations on melting and solidification processes in phase change materials. Applied Thermal Engineering, 2025; 258: 124726. https://doi.org/10.1016/j.applthermaleng.2024.124726
- [23] Naldi C, Martino G, Dongellini M, Lorente S. Rayleigh-Bénard type PCM melting and solid drops. International Journal of Heat and Mass Transfer, 2024; 218: 124767. https://doi.org/10.1016/j.ijheatmasstransfer.2023.124767
- [24] Stritih U. An experimental study of enhanced heat transfer in rectangular PCM thermal storage. International Journal of Heat and Mass Transfer, 2004; 47: 2841-2847. https://doi.org/10.1016/j.ijheatmasstransfer.2004.02.001